Journal of Alloys and Compounds 499 (2010) 90–97

Contents lists available at ScienceDirect

Journal of Alloys and Compounds

journal homepage: www.elsevier.com/locate/jallcom

High pressure phase-transition, elastic and thermal properties of uranium chalcogenides: A model study

Dinesh Chandra Gupta[a,*], Ashok Kumar Baraiya[a,b]

[a] Condensed Matter Theory Group, School of Studies in Physics, Jiwaji University, Gwalior 474 011, India
[b] Department of Physics, SMS Government Science College, Gwalior 474 002, India

ARTICLE INFO

Article history:
Received 27 October 2009
Received in revised form 3 March 2010
Accepted 3 March 2010
Available online 11 March 2010

Keywords:
High pressure phase transition
Equation of state
Elastic properties
Thermophysical properties

ABSTRACT

Uranium chalcogenides crystallize in $Fm\bar{3}m$ space group at ambient condition and transform to $Pm\bar{3}m$ space group under pressure. We have investigated the elastic and thermo-physical properties of uranium mono-chalcogenides using modified charge-transfer potential model. This model incorporates long-range Coulomb effects and charge-transfer (Coulomb screening due to f-electrons of U) effect modified by covalency and short-range repulsive interaction extended up to next-nearest neighbours. This model is capable of explaining the Cauchy-discrepancy. Calculated values of the phase-transition pressure (P_T = 79.50, 19.60 and 9.50 GPa) and relative volume collapse (4.69, 7.95 and 7.88%) are in good agreement with experimental data. The equation of state has been plotted to get phase diagram.

1. Introduction

The uranium compounds (UX, X = N, P, As, Sb, S, Se, Te) crystallize in rock-salt structure and show wide variety of anomalous behaviour, so far as their elastic and phase transition [1–9], phonon [10–13], electronic [14,15] and magnetic [16,17] properties are concerned. A review on this type of study is reported by Benedict [1]. Rigid ion model (RIM) and shell model (SM) with two-body interaction have been employed by Jha and Sanyal [10] to study the phonon properties of uranium compounds while Srivastava et al. [18] have used a two-body potential to study the phase transition properties, which is not adequate for explaining the Cauchy-violation ($C_{12} \neq C_{44}$) in the elastic constants. It may also be noted that the values of ΔG shown by them in Figs. 1–3a and Table 3 differ from each other and hence their results are not reliable. Uranium mono-chalcogenides (US, USe and UTe) have rock-salt (B1) structure with f-electrons and metallic conductivity. These compounds undergo pressure induced structural transformation from sixfold coordinated B1 phase to eightfold coordinated $Pm\bar{3}m$ (B2) structure. From simple valence considerations, they have $5f^3 6d^1$ configuration. The fluctuation of f-electrons in rare-earth atoms under pressure is a striking feature and makes them an interesting family of rare-earth compounds. Besides structural transformation, they also show f-electron fluctuation [19]. Moreover, since uranium compounds with large lattice constants and narrow f-bands, the coupling between the discrete $6d \rightarrow 5f$ atomic excitation and the continuum states may turn out to be an important method of studying the degree of 5f delocalization. The electronic structure study of these compounds reveals that localized core and delocalized f-electrons are responsible for this valence fluctuation. Under applied external pressure, this nature of f-orbital can be tuned [19–21]. Uranium compounds, besides being used in reactors technology, possess several interesting and controversial properties. Hence, over last two decades they have attracted the attention of both experimental and theoretical physicists. These chalcogenides (UX, X = S, Se Te) show ferromagnetic ordering while their pnictides (UY, Y = N, P, As, Sb, Bi) are ordered antiferromagnetically. The detailed study of lattice vibrational properties of these compounds has been reported by Durai and Babu [22].

Recently, Gour et al. [23], Varshney et al. [24–27] and Srivastava et al. [18] have computed various crystal properties of Eu- and U-compounds but many of these, especially elastic properties and Cauchy-discrepancy and their pressure variation are not explained well due to the exclusion of covalency and many-body interactions (MBI) in the expressions of elastic moduli. These interactions are responsible for the Coulomb screening effect due to the delocalized f-electrons in rare-earth ion. The inclusion of covalency effect is expected to improve the prediction of the crystal properties under high pressure because it increases with pressure.

In the present article, we have developed an improved potential model, which incorporates proper crystal interactions *viz.*, long-range (LR) Coulomb attraction and Coulomb screening due to f-electrons of rare-earth ion/atom (charge-transfer or many-body interaction (CTI or MBI)) modified by covalency effects [28] and short-range (SR) repulsion extended up to second nearest neighbours and represented by Hafemeister and Flygare (HF) type

* Corresponding author. Tel.: +91 751 2442777; fax: +91 751 2442784/2442787.
E-mail addresses: sosfizix@yahoo.co.in, sosfizix@gmail.com (D.C. Gupta).

0925-8388/$ – see front matter © 2010 Elsevier B.V. All rights reserved.
doi:10.1016/j.jallcom.2010.03.059

potential [29] since these compounds are partially covalent in nature. Although, the model used by Gour et al. [23], Varshney et al. [24–27] and Srivastava et al. [18] are basic for explaining crystal properties but they does not include covalency effect, which plays an important role in defining the crystal properties of these heavy-earth compounds (HECs). Hence, their approach is not realistic qualitatively and quantitatively. For the present computations, we used the corrected/modified expressions of the second-order elastic constants (SOECs), their combination, Cauchy's discrepancy, third-order elastic constants (TOECs) and first- and second-order pressure derivatives of SOECs as reported in the next section.

2. Modified potential model

Under compression, the outer most electronic shells of the adjacent ions/atoms overlap. This gives rise to charge-transfer/many-body interactions. The potential energy thus maybe written as the sum of the following terms:

The LR Coulomb attraction

$$U_{\mathrm{COUL}}(r) = -\frac{\alpha_{\mathrm{M}} Z^2 e^2}{r_{kk'}}$$

with α_{M} as Madelung constants, Ze as ionic charge and $r_{kk'}$ as interionic separation which is equal to r_{o} at equilibrium.

The LR Coulomb screening due to the delocalization of the f-electron of rare-earth ion/atom or charge-transfer interactions (CTI) modified by covalency effects is expressed as

$$U_{\mathrm{MCTI}}(r) = -2n\alpha_{\mathrm{M}} e^2 Z \frac{f_{\mathrm{m}}(r_{kk'})}{r_{kk'}}$$

Here, n is the number of nearest-neighbours and $f_{\mathrm{m}}(r_{kk'})$ is the charge-transfer parameter incorporating covalency effect.

The SR overlap repulsive potential extended up to second neighbouring ions is given by HF [29] as

$$U_{\mathrm{HF}} = b\sum_{kk'} \beta_{kk'} \exp\left(\frac{r_k + r_{k'} - r_{kk'}}{\rho}\right)$$

Here, r_k and $r_{k'}$ are the radii of anion and cation, respectively, $\beta_{kk'}$ is Pauling's coefficient for k–k', k–k and k'–k' interactions. $r_{kk} = r_{k'k'} (= r_{\mathrm{o}}\sqrt{2})$ is the next-nearest neighbour distance, b is hardness parameter while ρ is range parameter. The $\beta_{kk'}$ is defined as

$$\beta_{kk'} = 1 + \frac{Z_k}{n_k} + \frac{Z_{k'}}{n_{k'}}$$

where Z_k ($Z_{k'}$) and n are the number of valence and the number of outermost electrons, respectively. Thus, the final expression of the modified charge-transfer potential (MCTP) model can be written as

$$U(r) = -\frac{\alpha_{\mathrm{M}} Z_{\mathrm{m}}^2 e^2}{r_{\mathrm{o}}} + b\sum_{kk'} \beta_{kk'} \exp\left(\frac{r_k + r_{k'} - r_{kk'}}{\rho}\right) \quad (1)$$

where $Z_{\mathrm{m}} e = \pm e(Z^2 + 2nZf_{\mathrm{m}}(r_{\mathrm{o}}))^{1/2}$ maybe interpreted as modified ionic charge $f_{\mathrm{m}}(r_{\mathrm{o}}) = f_{\mathrm{CTI}}(r_{\mathrm{o}}) + f_{\mathrm{COV}}(r_{\mathrm{o}})$ with $f_{\mathrm{CTI}}(r_{\mathrm{o}}) = f_{\mathrm{o}} e^{-r_{\mathrm{o}}/\rho}$ and $f_{\mathrm{COV}}(r) = (4V_{\mathrm{sp}\sigma}^2 e^2 / r_{\mathrm{o}} E_{\mathrm{g}}^3)(1 - (e_{\mathrm{s}}^*/e))$ with $(V_{\mathrm{sp}\sigma}^2/E_{\mathrm{g}}) = (1 - (e_{\mathrm{s}}^*/e))/12$ and $E_{\mathrm{g}} = E - I + e^2((2\alpha_{\mathrm{M}} - 1)/r_{\mathrm{o}})$.

Here, E_{g} is the transfer energy of electron from anion to cation, E denotes the electron affinity of the cation and I the ionization potential of the rare-earth atom. Further,

$$(e_{\mathrm{s}}^*)^2 = \frac{9V\omega_{\mathrm{T}}^2(\varepsilon_0 - \varepsilon_\infty)}{4\pi N(\varepsilon_\infty + 2)^2} \quad \text{and} \quad \left(\frac{e_{\mathrm{s}}^*}{e}\right)^2 = \frac{9V\mu\omega_{\mathrm{o}}^2(\varepsilon_0 - \varepsilon_\infty)}{4\pi e^2(\varepsilon_\infty + 2)^2}$$

with V as the volume of the unit cell. ε_0 and ε_∞ are the static and optic dielectric constants while μ denotes the reduced mass of the ions and ω_{o} the infrared frequency. To solve them we have used Lydanne-Sachs and Teller (LST) relation [30] $(\omega_{\mathrm{L}}^2/\omega_{\mathrm{T}}^2) = (\varepsilon_0/\varepsilon_\infty)$ with ω_{L} and ω_{T} as longitudinal and transverse frequencies at zone center.

The values of the model parameters, *viz.* b, ρ and $f_{\mathrm{m}}(r)$ have been computed from the knowledge of the compressibility or the bulk modulus and equilibrium conditions as described by Gupta and Singh [31] using the self-consistent method of minimization of the cohesive energy $(\mathrm{d}U/\mathrm{d}r)\big|_{r=r_{\mathrm{o}}} = 0$ or $B_1 + B_2 = -1.165 Z_{\mathrm{m}}^2$ and $(\mathrm{d}^2U/\mathrm{d}r^2)\big|_{r=r_{\mathrm{o}}} = 9KrB_{\mathrm{T}}$ with $K(=V/r^3)$ as structure dependent constant.

Employing the methodology [32] of deriving the elastic constants, we have obtained the modified expressions of elastic moduli, their combinations and the first- and second-order pressure derivatives of SOECs and TOECs which are capable of explaining the Cauchy-discrepancy correctly.

The relative stability of the two competitive phases maybe expressed through $\Delta G(= G_{B_2} - G_{B_1})$, where G_{B1} and G_{B2} are the Gibbs free (GF) energies of the parent (B1) and transformed phase (B2). The GF energy for parent phase is expressed as

$$G_{\mathrm{B1}}(r) = U_{\mathrm{B1}}(r) + PV_{\mathrm{B1}} \quad (2)$$

While for transformed hypothetical B2 phase as

$$G_{\mathrm{B2}}(r') = U_{\mathrm{B2}}(r') + PV_{\mathrm{B2}} \quad (3)$$

Here, $U_{\mathrm{B1}}(r)$ and $U_{\mathrm{B2}}(r')$ are internal energies of rock-salt (B1) and cesium chloride (B2) phases which are expressed as

$$U_{\mathrm{B1}}(r) = -\frac{\alpha_{\mathrm{M}} Z_{\mathrm{m}}^2 e^2}{r_{\mathrm{o}}} + b\sum_{kk'} \beta_{kk'} \exp\left(\frac{r_k + r_{k'} - r_{kk'}}{\rho}\right) \quad (4)$$

$$U_{\mathrm{B2}}(r') = -\frac{\alpha'_{\mathrm{M}} Z_{\mathrm{m}}^2 e^2}{r_{\mathrm{o}}} + b\sum_{kk'} \beta_{kk'} \exp\left(\frac{r_k + r_{k'} - r'_{kk'}}{\rho}\right) \quad (5)$$

Here, the symbols in the above expressions have their usual meaning. The model parameters have been used for computing the phase-transition properties of the present set of HECs. The present modified charge-transfer potential (MCTP) model has been used to derive the expressions of the elastic moduli and other properties.

2.1. Second-order elastic constants for NaCl structure

The modified expressions for SOECs from the present model are given as

$$C_{11} = \frac{e^2}{4a^4}\left[-5.112\ Z_{\mathrm{m}}^2 + A_1 + \frac{A_2 + B_2}{2} + \underline{9.3204\ Zaf'(r_{\mathrm{o}})}\right] \quad (6)$$

$$C_{12} = \frac{e^2}{4a^4}\left[0.226 Z_{\mathrm{m}}^2 - B_1 + \frac{A_2 - 5B_2}{4} + \underline{9.3204\ Zaf'(r_{\mathrm{o}})}\right] \quad (7)$$

$$C_{44} = \frac{e^2}{4a^4}\left[2.556 Z_{\mathrm{m}}^2 + B_1 + \frac{A_2 + 3B_2}{4}\right] \quad (8)$$

with equilibrium condition

$$B_1 + B_2 = -1.165 Z_{\mathrm{m}}^2 \quad (9)$$

Using Eq. (9), we can rewrite the above Eqs. (7) and (8) as

$$C_{12} = \frac{e^2}{4a^4}\left[1.391 Z_{\mathrm{m}}^2 + \frac{A_2 - B_2}{4} + \underline{9.3204\ Zaf'(r_{\mathrm{o}})}\right] \quad (7a)$$

$$C_{44} = \frac{e^2}{4a^4}\left[1.391 Z_{\mathrm{m}}^2 + \frac{A_2 - B_2}{4}\right] \quad (8a)$$

We wish to point out that the results obtained by Gour et al. [23], Varshney et al. [24–27] and Srivastava et al. [18] actually lead to $C_{12} = C_{44}$ while their results show $C_{12} \neq C_{44}$. It is clear from the above derivations that our analysis naturally expresses the Cauchy-discrepancy ($C_{12} - C_{44} \neq 0$) [as underlined in Eq. (7a)] in terms

of CTI parameter. The relation for Cauchy-discrepancy from the present expressions comes out to be

$$C_{12} - C_{44} = 9.3204\ Z\frac{e^2}{4a^4}af'(r_o) \tag{10}$$

2.2. Second-order elastic constants for CsCl structure

Similarly, we have also derived the modified expressions for SOECs from the present model for CsCl structure as

$$C_{11} = \frac{e^2}{4a^4}\left[0.7009Z_m^2 + A_1 + \frac{A_2+2B_2}{6} + \frac{A_2}{2} + \underline{3.1337\ Zaf'(r_o)}\right] \tag{11}$$

$$C_{12} = \frac{e^2}{4a^4}\left[-0.6897\ Z_m^2 + \frac{A_1-4B_1}{6} - \frac{B_2}{2} + \underline{3.1337\ Zaf'(r_o)}\right] \tag{12}$$

$$C_{44} = \frac{e^2}{4a^4}\left[-0.3504Z_m^2 + B_1 + \frac{A_1+2B_1}{6} + \frac{B_2}{2}\right] \tag{13}$$

with

$$B_1 + B_2 = -0.3392Z_m^2 \tag{14}$$

as equilibrium condition.

For cubic structure with B1 phase, the necessary conditions for mechanical stability have been given elsewhere [33] as

$$(C_{11} - C_{12}) > 0, \quad (C_{11} + 2C_{12}) > 0 \quad \text{and} \quad C_{11} > 0, \quad C_{44} > 0 \tag{15}$$

It maybe noticed that if we ignore the correction term from the expression of C_{12}, we get $C_{12} = C_{44}$, which is not correct. We have also derived the expressions for TOECs and the first- and second-order pressure derivatives of SOECs. The correction terms have been underlined in these expressions. The underlined terms in the above expressions have been omitted by Gour et al. [23] and Varshney et al. [24–27] while Srivastava et al. [18] have considered two-body potential which naturally ignores the many-body interactions.

Based on these SOECs, we have also computed various other mechanical properties, which explain strength and nature of the material for different applications, of these compounds. The shear (C_S) and stiffness constant (C_L) is given by:

$$C_S = \frac{C_{11} - C_{12}}{2} \quad \text{and} \quad C_L = \frac{C_{11} + C_{12} + 2C_{44}}{2} \tag{16}$$

Another important parameter is the Kleinman parameter [34]

$$\xi = \frac{C_{11} + 8C_{12}}{7C_{11} + 2C_{12}} \tag{17}$$

which describes the relative positions of the cation and anion sub-lattices under volume conserving strain distortions for which positions are not fixed by symmetry.

The isotropic bulk modulus and shear modulus for cubic system are given as

$$B_0 = \frac{C_{11} + 2C_{12}}{3} \quad \text{and} \quad G = \frac{C_{11} - C_{12} + 3C_{44}}{5} \tag{18}$$

From the SOECs, two parameters having a substantial and geophysical interest can be examined. They are elastic anisotropy factor (A) and the Cauchy's relation defined as

$$A = \frac{2C_{44}}{C_{11} - C_{12}} \tag{19}$$

The Cauchy relation $C_{12} - C_{44} = 2P$ (P: pressure) is valid only when all interatomic forces are composed by two-body central interactions under static lattice conditions.

We have also obtained the values of the Young's modulus (Y) and Poisson's ratio (σ). These quantities are related to the isotropic bulk modulus (B_0) and the shear modulus (G) by the following equations

$$Y = \frac{9B_0G}{3B_0 + G} \quad \text{and} \quad \sigma = \frac{3B_0 - Y}{6B_0} \tag{20}$$

2.3. Third-order elastic constants

The expressions for TOECs derived from the present MCTP model are

$$C_{111} = \frac{e^2}{4a^4}\left[37.563\ Z_m^2 + C_1 - 3A_1 + \frac{C_2 - 3A_2 - C_2}{4} - \underline{89.304\ Zaf'(r_o)} + \underline{13.981Za^2f''(r_o)}\right] \tag{21}$$

$$C_{112} = \frac{e^2}{4a^4}\left[-4.836\ Z_m^2 - \frac{3A_2 - 3B_2 - C_2}{8} - \underline{18.64\ Zaf'(r_o)} + \underline{4.66Za^2f''(r_o)}\right] \tag{22}$$

$$C_{123} = \frac{e^2}{4a^4}\left[2.717\ Z_m^2 + \underline{16.692Zaf'(r_o)}\right] \tag{23}$$

$$C_{144} = \frac{e^2}{4a^4}\left[2.717\ Z_m^2 + 5.564Zaf'(r_o)\right] \tag{24}$$

$$C_{166} = \frac{e^2}{4a^4}\left[-9.496Z_m^2 - \frac{(3A_2 - 3B_2 - C_2)}{8} + \underline{5.564Zaf'(r_o)}\right] \tag{25}$$

$$C_{456} = \frac{e^2}{4a^4}\left[2.717Z_m^2\right] \tag{26}$$

Here, A_1, B_1, C_1, A_2, B_2, and C_2 are SR parameters due to the nearest and next-nearest neighbours and can be evaluated with the help of the following expressions

$$B_1 = \left(\frac{4a^2}{e^2}\right)\left[\frac{\partial V_1(r)}{\partial r}\right]_{r=a} \tag{27}$$

$$A_1 = \left(\frac{4a^3}{e^2}\right)\left[\frac{\partial^2 V_1(r)}{\partial r^2}\right]_{r=a} \tag{28}$$

$$C_1 = \left(\frac{4a^4}{e^2}\right)\left[\frac{\partial^3 V_1(r)}{\partial r^3}\right]_{r=a} \tag{29}$$

$$D_1 = \left(\frac{4a^5}{e^2}\right)\left[\frac{\partial^4 V_1(r)}{\partial r^4}\right]_{r=a} \tag{30}$$

$$B_2 = \left(\frac{8a^2}{e^2}\right)\left[\frac{\partial V_2(r)}{\partial r}\right]_{r=a\sqrt{2}} \tag{31}$$

$$A_2 = \left(\frac{8a^3}{e^2}\right)\left[\frac{\partial^2 V_2(r)}{\partial r^2}\right]_{r=a\sqrt{2}} \tag{32}$$

$$C_2 = \left(\frac{8a^4}{e^2}\right)\left[\frac{\partial^3 V_2(r)}{\partial r^3}\right]_{r=a\sqrt{2}} \tag{33}$$

$$D_2 = \left(\frac{8a^5}{e^2}\right)\left[\frac{\partial^4 V_2(r)}{\partial r^4}\right]_{r=a\sqrt{2}} \tag{34}$$

with $V_1(r)$ and $V_2(r)$ as the overlap repulsive potentials due to the nearest and next-nearest neighbours

$$V_1(r) = b\beta_{kk'}\ \exp\left(\frac{r_k + r_{k'} - r_o}{\rho}\right) \tag{35}$$

$$V_2(r) = b\left[\beta_{kk}\exp\left(\frac{2r_k - r_o\sqrt{2}}{\rho}\right) + \beta_{k'k'}\exp\left(\frac{2r_{k'} - r_o\sqrt{2}}{\rho}\right)\right] \quad (36)$$

where r_k and $r_{k'}$ are radii of anion and cation with r_o as interionic separation.

2.4. First- and second-order pressure derivatives of SOECs

The expressions for first- and second-order pressure derivatives of bulk ($B_T = (C_{11} + 2C_{12})/3$), shear moduli ($C_S = (C_{11} - C_{12})/2$) and C_{44} for NaCl structure are given below

$$\frac{dB_T}{dP} = -\frac{1}{3\eta}[13.98\ Z_m^2 - 3(A_1 + A_2) + C_1 + C_2 - \underline{167.765\ Zaf'(r_o)} + \underline{41.942\, Za^2 f''(r_o)}] \quad (37)$$

$$\frac{dC_S}{dP} = -\frac{1}{2\eta}\left[23.682\, Z_m^2 + C_1 + \frac{6A_2 - 6B_2 + C_2}{4} - \underline{50.075\, Zaf'(r_o)} + \underline{13.981\, Za^2 f''(r_o)}\right] \quad (38)$$

$$\frac{dC_{44}}{dP} = -\frac{1}{\eta}\left[-7.894\, Z_m^2 + A_1 + \underline{44.653\, Zaf'(r_o)} + \frac{2A_2 + 2B_2 + C_2}{4}\right] \quad (39)$$

where $\eta = 2.33\, Z_m^2 + A_1 + A_2 + \underline{27.961\, Zaf'(r_o)}$

Upon differentiating Eqs. (37)–(39) with respect to pressure (P), we get expressions for the second-order pressure derivatives of elastic moduli as

$$\frac{d^2B_T}{dP^2} = \frac{w}{3}\left[-65.24\ Z_m^2 + 7(A_1 + A_2) - 3(C_1 + C_2) + D_1 + D_2 + \underline{782.898\ Zaf'(r_o)} - \underline{293.591\, Za^2 f''(r_o)} + \underline{55.923\, Za^3 f'''(r_o)} + \frac{3dB_T}{dP}\left\{13.98\ Z_m^2 - 3(A_1 - A_2) + C_1 + C_2 - \underline{167.765\, Zaf'(r_o)} + \underline{41.942\, Za^2 f''(r_o)}\right\}\right] \quad (40)$$

$$\frac{d^2C_S}{dP^2} = \frac{w}{2}\left[-90.068\, Z_m^2 - 2A_1 + D_1 - 5A_2 + 3B_2 + \frac{6C_2 + D_2}{4} + \underline{378.487\ Zaf'(r_o)} - \underline{78.037\, Za^2 f''(r_o)} + \underline{27.962\, Za^3 f'''(r_o)} + \frac{3dB_T}{dP}\left\{23.682 Z_m^2 + C_1 + \frac{6A_2 - 6B_2 + C_2}{4} - \underline{50.075\, Zaf'(r_o)} + \underline{13.981\, Za^2 f''(r_o)}\right\}\right] \quad (41)$$

$$\frac{d^2C_{44}}{dP^2} = w\left[-45.556\, Z_m^2 - 3A_1 + C_1 - 2A_2 - B_2 + \frac{2C_2 + D_2}{4} - \underline{284.608\, Zaf'(r_o)} + \underline{58.634\, Za^2 f''(r_o)} + \frac{3dB_T}{dP}\left\{-7.894 Z_m^2 + \frac{2A_2 + 2B_2 + C_2}{4} + A_1 + \underline{44.653\ Zaf'(r_o)}\right\}\right] \quad (42)$$

where $w = a^2 e\beta_T/36$.

The higher derivatives of the CTI parameter $f(r_o)$, i.e., $af'(r_o)$, $a^2f''(r_o)$ and $a^3f'''(r_o)$ have been evaluated from the analytical expression $f_m(r_o) = f_o\exp(-r/\rho)$ as suggested by Cochran [35].

3. Computation of model parameters

The modified MCTP model consists of only three parameters, namely, hardness (b), range (ρ) and modified CTI parameter ($f_m(r_o)$). These values have been calculated from the self-consistent method using the compressibility or bulk modulus and equilibrium conditions as described by Gupta and Singh [31]. The values of the input data along with the computed model parameters are listed in Table 1.

Table 1
Input data r_o in (10^{-10} m), B_T in (GPa) and model parameters b in (10^{-19} J), ρ in (10^{-10} m) for uranium chalcogenides.

Solids	Input data		Model parameters		
	r_o	B_T	b	ρ	f_o
US	2.7475[b]	105[a]	11.99	0.3213	225.08
USe	2.8720[b]	74[a]	41.73	0.3137	214.14
UTe	3.0775[b]	48[a]	103.90	0.3050	118.07

[a] Ref. [1].
[b] Ref. [17].

4. Results and discussion

4.1. Phase transition properties

In order to check the relative stability of the two competitive phases, we have minimized the lattice energies in both the real and the hypothetical phases at ambient conditions corresponding to equilibrium interionic separation $r(r')$ using the MCTP model parameters listed in Table 1. The corresponding GF energies $G_{B1}(r)$ and $G_{B2}(r')$ have been computed at difference pressures. The GF energy difference $\Delta G[= G_{B2}(r') - G_{B1}(r)]$ has been computed and plotted as a function of pressure in Fig. 1 to obtain the phase transition pressure (P_T). The pressure at which ΔG becomes zero has been marked by arrows in these figures as P_T and their values are reported in Table 2 along with available measured data and compared with earlier theoretical results. It is seen that the value of ΔG at zero pressure is positive in all the cases which is the required criterion for relative stability of the two competitive phases. The present MCTP model thus predicts correctly that B1 phase is thermodynamically and mechanically stable at ambient conditions. The value of ΔG remains positive up to just before P_T and becomes zero at P_T exhibiting the coexistence of both the phases at this pressure. The values of P_T computed by us are in good agreement with the experimental results [1,6] and better than those obtained by earlier workers [18,24]. ΔG becomes negative beyond P_T predicting thereby that the high pressure B2 phase is now thermodynami-

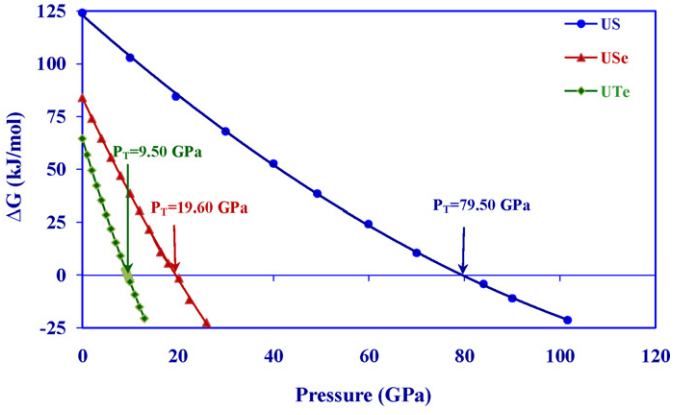

Fig. 1. Variation of Gibbs free energy difference (ΔG) with pressure for U-chalcogenides.

Table 2
Calculated values of Gibbs free energy difference (ΔG in kJ/mol), phase transition pressure (P_T in GPa) and % of volume collapse at P_T ($\Delta V(P_T)/V(0)$) for uranium chalcogenides.

Solids	r_{B1}	ΔG	P_T	% $V(P_T)/V(0)$	Ref.
US	2.7472	124.17	79.50	4.69	Present
	2.7475		80.00	–	Expt. [2]
	–		81.00	4.70	Other [24]
	2.4098		78.5	5.4	Other [18]
USe	2.8717	84.04	19.60	7.95	Present
	2.8720[a]		20.00	8	Expt. [1]
	–		21.00	7.00	Other [24]
	2.6946		21	10.3	Other [18]
UTe	3.0763	64.54	9.50	7.88	Present
	3.0775		9.00	8	Expt. [1]
	–		13.00	5.60	Other [24]
	2.9282		9.5	11.3	Other [18]

[a] Ref. [2].

cally and mechanically stable as compared to parent B1 phase. It is observed that the value of the P_T decreases from S to Te through Se (i.e., as the ionic size and atomic number increases).

In Fig. 2, we have plotted the variation of modified ionic charge (Z_m^2) with lattice constant of uranium compounds. It decreases with increase of lattice constant. Furthermore, the observed value of negative gradient of Z_m^2 is a direct consequence of a decreasing trend of variation in bulk modulus as is evident from Table 1. The large value of bulk modulus for US shows strong ionic character in it as compared to other members of the series. However, the small value of Z_m^2 for USe and UTe indicates strong delocalization of f-electrons in them, i.e., the linear trend of Z_m^2 in the present series of compounds (US > USe > UTe) can be interpreted as the competition between localization of the U 5f states and the f–p hybridization. Our discussion of valency implies that there is a direct relationship between the difference in the number of the less well localized f electrons and the difference in energy between the two valence states.

The self-consistently computed values of interionic distances have been used to compute the ratio of volume at pressure ($V(P)$) to the volume at ambient pressure ($V(0)$). These values of the reduced volume ($V(P)/V(0)$) in different phases have been plotted in Fig. 3(a–c) to obtain the equation of state (EOS)/phase diagram and in consequence the percentage volume collapse ($V(P_T)/V(0)$) at P_T. These values along with the GF energy difference (ΔG), phase transition pressure (P_T) have been reported in Table 2. All the three compounds are found to be stable B1 phase with lowest GF energy as compared to that in B2 phase. Our data shows B1–B2 structural phase transition at 79.50, 19.60 and 9.50 GPa with volume collapse of 4.69, 7.95 and 7.88% for US, USe and UTe, respectively. Our computed values of P_T and volume collapse are in good agreement with

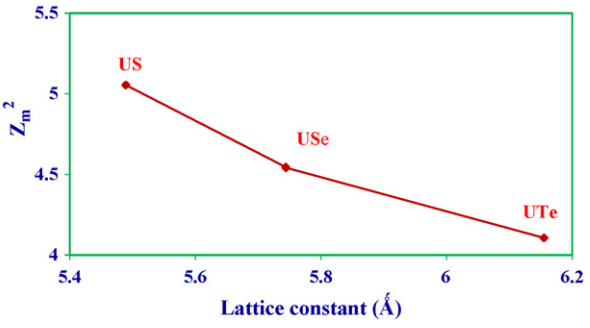

Fig. 2. Variation of effective ionic charge Z_m^2 with lattice constant for U-chalcogenides.

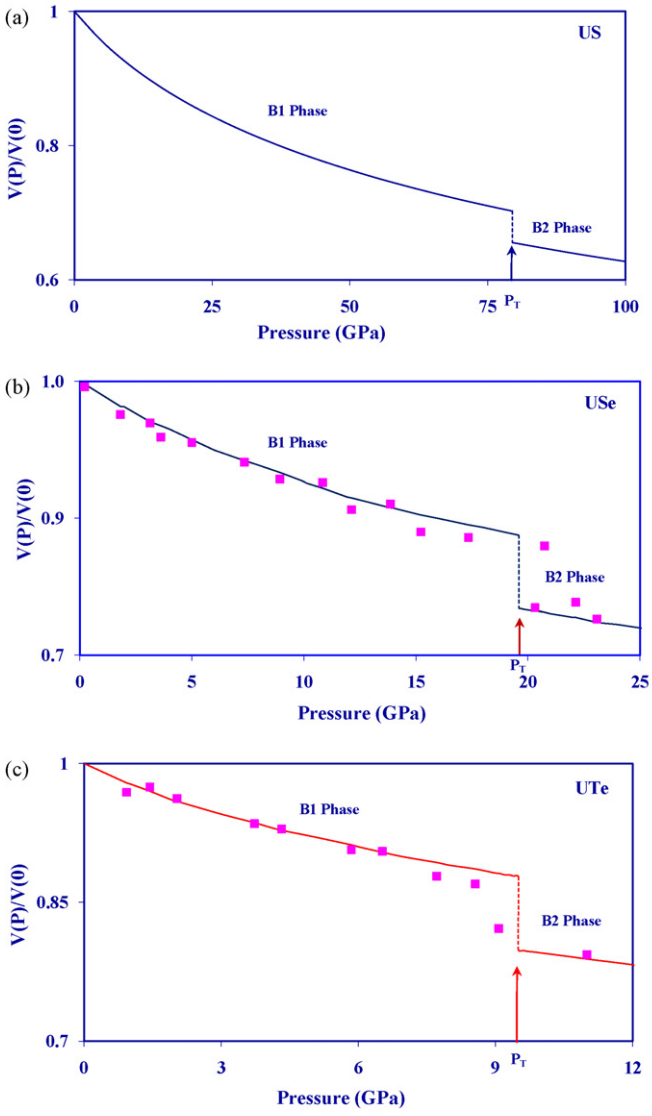

Fig. 3. Variation of reduced volume with pressure for (a) US, (b) USe and (c) UTe. Experimental points (■) are taken from Ref. [19].

the experimental results [1,2] and better than those obtained by others [18,24].

In Fig. 4, we have shown the variation of U–U and U–X (X = S, Se and Te) distance with pressure for these compounds. In US the distance between U and S is 2.7445 Å at the ambient condition. The bond between U and S is found to be partially covalent in nature. The U–S distance is larger than the sum of covalent radii of U (0.80 Å) and S (1.24 Å) and smaller than the sum of atomic radius of U (1.385 Å) and covalent radius of S (1.02 Å). It is also clear that the value of nearest neighbour distance shows an abrupt decline at P_T while the next-nearest neighbour distance increases abruptly at P_T. This increase in interionic distance gives rise to weakening of Coulomb force in CsCl phase and it is counteracted by nearest neighbour repulsive forces. The SR repulsion due to next-nearest neighbours also shows decrease with pressure. Similar trend is found in other compounds of this family.

4.2. Elastic properties

To study the mechanical strength of these compounds, we have computed SOECs and their combinations (C_L, C_S and B_T) at ambient as well as at high pressure conditions, ξ, B_0, G, A, Y and Chauchy's

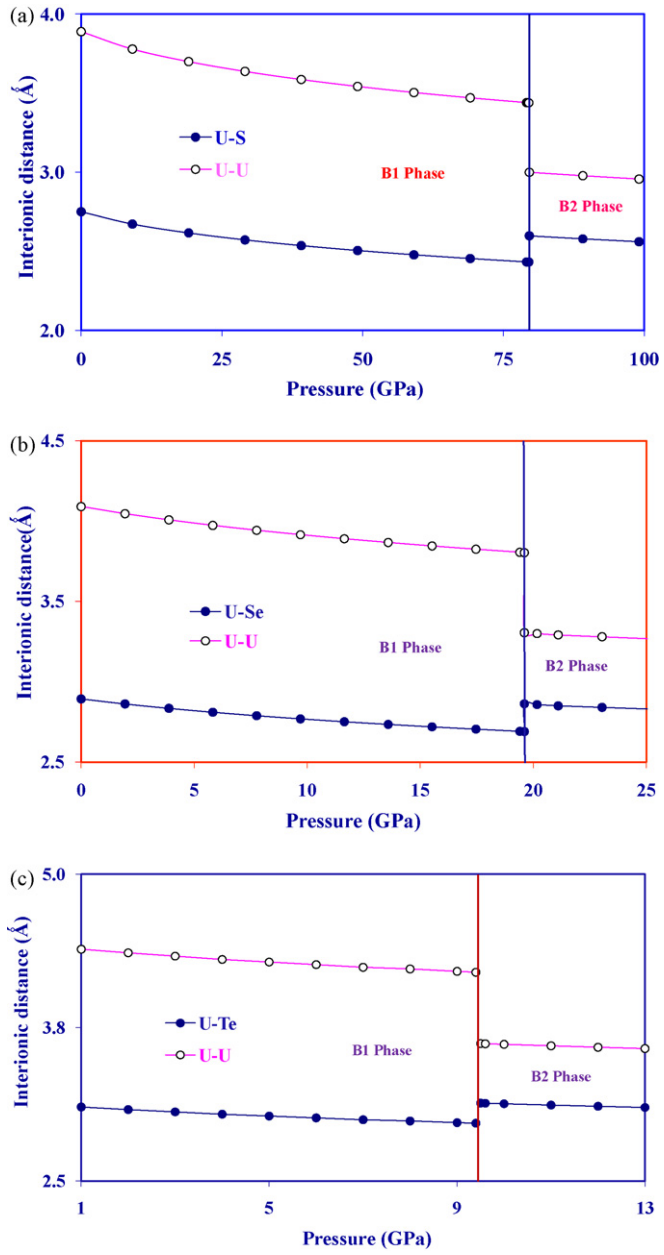

Fig. 4. Variation of interionic distance with pressure of U–U and U–X; (a) U–S, (b) U–Se (c) U–Te.

discrepancy, σ, TOECs and the first- and second-order pressure derivatives of SOECs for US, USe and UTe, respectively. Their values in B1 phase have been reported in Table 3. The values of SOECs satisfy all the stability conditions given earlier and hence it maybe conclude that these compounds are mechanically stable in the B1 phase. It maybe seen from Table 3 that the present theoretical values of SOCEs and their combinations are close to the measured data and better than those obtained by others [18,24]. The value of Cauchy's discrepancy at zero pressure is negative which indicates violation of the Cauchy's relation. These values decrease with the size of chalcogen atom from S → Te in B1 phase. This shows that the non-central character of the forces, implicit in the Cauchy's relation increase with the decrease of lattice constant. The negative Cauchy's discrepancy is a consequence of the hybridization of the unstable f band, which maybe responsible for the decrease in U–U distance thereby to small value of elastic constant C_{12}. The elastic anisotropic factor (A) used in the interpretation of the seismological

Table 3
Calculated values of elastic moduli and their combinations (in GPa) for uranium compounds at ambient condition.

Property	US	USe	UTe	Ref.
C_{11}	186.70	128.48	104.87	Present
	245 ± 14	–	–	Expt. [3]
	301.7 ± 10.39	–	143.4 ± 3.60	Expt. [4]
	–	194 ± 14	149 ± 3	Expt. [5]
	305 ± 15	–	–	Expt. [6]
	125.69	101.23	48.03	Other [18]
	119.00	60.00	2.00	Other [24]
C_{12}	97.27	25.12	6.05	Present
	4 ± 7	–	–	Expt. [3]
	13.2 ± 7.3	–	–	Expt. [4]
	–	0.0 ± 7	−20 ± 4	Expt. [5]
	70.51	58.97	46.16	Other [18]
	39.00	4.00	0.02	Other [24]
C_{44}	71.23	35.13	22.58	Present
	21 ± 1	–	–	Expt. [3]
	16.93 ± 0.19	–	12 ± 0.2	Expt. [4]
	–	16 ± 1	11.3 ± 0.4	Expt. [5]
	17.2 ± 0.5	–	–	Expt. [6]
	73.81	61.80	49.47	Other [18]
	55.00	22.00	19.00	Other [24]
B_T	107.1	59.57	38.99	Present
	105	74	48	Expt. [1]
	84 ± 6	–	–	Expt. [3]
	107 ± 8	–	–	Expt. [4]
	–	65 ± 7	34 ± 6	Expt. [5]
	66.00	23.00	0.70	Other [24]
C_S	59.71	51.68	49.41	Present
	144.25	–	–	Expt. [4]
	–	97.00	84.50	Expt. [5]
	40.00	28.00	1.00	Other [24]
C_L	198.22	111.94	78.08	Present
	174.38	–	–	Expt. [4]
	–	113.00	75.80	Expt. [5]
	134.00	54.00	20.01	Other [24]
A	1.19	0.67	0.45	Present
	0.17[a]	0.17[c]	0.14[b]	Expt.
G	66.62	41.75	33.31	Present
	63.6[a]	42.2[c]	32.58[c]	Expt.
σ	0.23	0.26	0.17	Present
	0.19[a]	0.23[c]	0.13[c]	Expt.
Y	165.51	102.32	77.78	Present
	152.34[a]	104.07[c]	74.07[c]	Expt.
ξ	0.50	0.34	0.20	Present
	0.16[a]	0.18[c]	-0.01[c]	Expt.
$C_{12} - C_{44}$	−2.88	−10.01	−19.53	Present
	−3.73[b]	−10.00[c]	−31.00[c]	Expt.
	−16.00	−18.00	−18.98	Other [24]

[a] Ref. [3].
[b] Ref. [4].
[c] Ref. [5].

and shear-wave velocities anisotropy as reported in Table 3 shows that these compounds are anisotropic (if "A" approaches unity the crystal becomes isotropic) but it is comparatively large as compared to others materials of rare-earth family [36]. The calculated values of Y, A, G and ξ decrease with increase of anion size. These values are close to the measured values [3–6] and follow the same trend in other compounds too. The values of σ are also close to experimental data and it first increase from S to Se and then decrease from Se to Te. Similar trend of variation is also shown by measured data. The overall improvement in the results is a consequence of proper consideration of interactions in defining the present interaction potential. The results are qualitatively and quantitatively better than the earlier results and support the modified expressions. The expressions of Gour et al. [23], Varshney et al. [24–27]

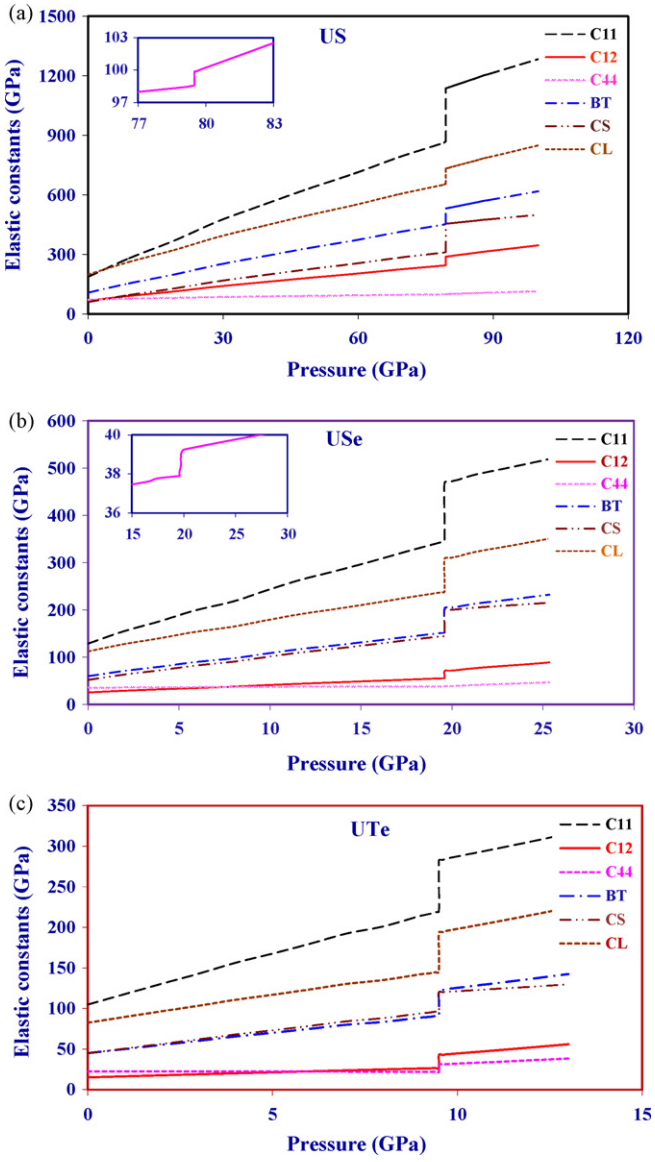

Fig. 5. Variation of SOECs and their combinations with pressure for (a) US, (b) USe and (c) UTe. In figures (a) and (b) a closer view of the variation of C_{44} is shown in the insight figure.

and Srivastava et al. [18] show that $C_{12} - C_{44} = 0$, while their results show different values of C_{12} and C_{44} and hence their results are not reliable.

In order to study the elastic strength of these materials under high pressures, we have computed the SOECs and their combinations in both parent (B1) and high pressure (B2) phases at different pressures and depicted them in Fig. 5(a–c). It is seen that these quantities vary linearly up to P_T followed by an abrupt increase at P_T and beyond it they again increase linearly. This suggests that under compression the crystal becomes elastically unstable and transforms to a new phase with minimum free energy. It is further seen that our calculated results agree well with experimental values and better than those reported by earlier theoretical workers [18,24]. It is seen that C_L and C_S increase linearly with pressure which is the characteristic of a first-order transition. The improvement in the prediction of these values shows the importance of the role of the Coulomb screening or modified CTI in the expressions of the elastic moduli. The variations of elastic moduli with material lattice constant have been plotted in Fig. 6. It is seen that these quantities decrease with increase in anion radius. This maybe attributed to the

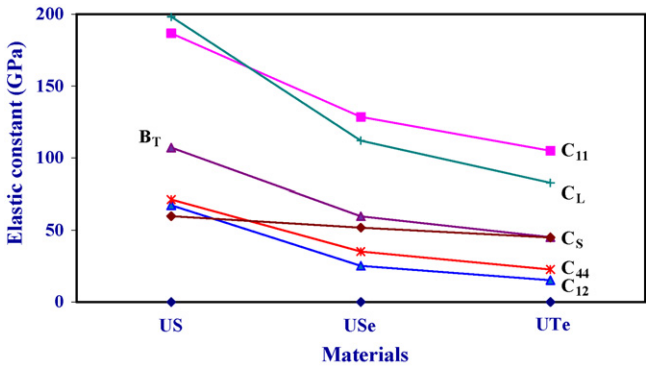

Fig. 6. Variation of SOECs with lattice parameter for uranium chalcogenides.

Table 4
Third-order elastic constants (10^2 GPa) of uranium chalcogenides.

Solids	C_{111}	C_{112}	C_{123}	C_{144}	C_{166}	C_{456}
US	−28.404	−3.010	0.890	0.953	−3.365	0.990
USe	−22.767	−0.969	0.379	0.478	−1.649	0.518
UTe	−19.931	−0.481	0.249	0.323	−1.030	0.354

increase in short-range repulsion due to nearest and next-nearest interaction forces with increase of anion size from S to Te via Se.

To compute the anhamonic properties of these compounds, we have calculated the values of TOECs and the pressure derivatives of the SOECs. The values of TOECs have been reported in Table 4 and the values of the pressure derivatives of the SOECs are reported in Table 5. It is seen from Table 4 that the C_{111}, C_{112} and C_{166} are negative for uranium chalcogenides and they increase with increase in the size of the chalcogen ion while the values of C_{123}, C_{144} and C_{456} are positive and they decrease with increasing size of the chalcogen ion. This might be due to the fact that the earlier quantities incorporate both LR attractive and SR repulsive forces in their expressions while the later expressions contain only LR attractive component. This trend of TOECs, in general, is consistent with the usual trend found in these compounds. It is also seen from this table that the values of all the TOECs decrease with increase in the size of chalcogen ion. It is seen from Table 5 that the values of first-order pressure derivatives of B_T, C_S and C_{44} are positive as found in most of the compounds with rock-salt structure. The value reported by Varshney et al. [24] for dC_{44}/dP is negative in all the three compounds which are unusual in the compounds with similar structure. But in the case of second-order pressure derivative, C_{44} is negative while B_T and C_S are positive. All the values of first- and second-order pressure derivatives increase with the increase of chalcogen ion except in the case of d^2C_{44}/dP^2 where it decreases. At present these values are of academic interest only and cannot be compared with other values due to non-availability of data.

Table 5
First- and second-order (10^{-22} GPa) pressure derivatives for uranium chalcogenides.

Property	US	USe	UTe	Ref.
dB_T/dP	3.05	3.42	3.75	Present
	4.06	3.52	2.96	Other [24]
dC_{44}/dP	0.38	0.244	0.07	Present
	−5.0	−0.57	−1.11	Other [24]
dC_S/dP	2.21	3.41	4.17	Present
	6.57	2.07	1.82	Other [24]
d^2B_T/dP^2	15.25	33.86	50.58	Present
d^2C_{44}/dP^2	−1.42	−3.28	−5.54	Present
d^2C_S/dP^2	12.94	36.50	60.05	Present

Table 6
The value of volume derivative of Poisson's ratio ($V(\mathrm{d}\sigma/\mathrm{d}V)$) in 10^{-24} GPa), α_v/C_v (in 10^{17} MKS units) Grüneisen parameter (γ) and Debye temperature (θ_D in K) for uranium chalcogenides.

Solids	US	USe	UTe	Ref.
$V(\mathrm{d}\sigma/\mathrm{d}V)$	0.1660	0.2525	0.3128	Present
α_v/C_v	4.102	3.662	2.006	Present
θ_D[a]	207.584	165.960	125.992	Present
	205 ± 2.5	172 ± 2.3	124 ± 2.5	Expt. [38]
	235	150	126	Other [24]
γ	2.4597	2.0514	1.9631	Present

[a] $\theta_D^3 = (3.15/8\pi)(h/k_B)^3(r/M)^{3/2}((C_{11}-C_{12})/2)^{1/2}((C_{11}+C_{12}+2C_{44})/2)^{1/2}C_{44}^{1/2}$ has been used.

4.3. Thermophysical properties

We have also computed the thermophysical properties of these compounds, i.e., volume derivative of Poisson's ratio ($V(\mathrm{d}\sigma/\mathrm{d}V)$), the ratio of thermal expansion coefficient to specific heat (α_v/C_v), Debye temperature (θ_D) and Grüneisen parameter (γ) for these compounds with the help of model parameters and the expressions reported elsewhere [37]. These values are reported in Table 6 and compared with available experimental data and others. It is clear that the values of θ_D and γ increase linearly while those of σ and $V(\mathrm{d}\sigma/\mathrm{d}V)$ decrease with the increase of ionic radii of chalcogen atom. Our values are more close to the measured values than the values reported by others [18,24].

5. Conclusions

In the present article, we have attempted to provide a unified picture of the crystal properties of uranium chalcogenides through MCTP model. For this purpose, we have developed an improved potential model which incorporates proper crystal interactions *viz*., long-range (LR) Coulomb and Coulomb screening effect due to the delocalization of f electrons of the rare-earth atom/ion (or charge-transfer/many-body interactions (CTI or MBI)) modified by covalency effects and short-range (SR) repulsion extended up to second nearest neighbours and represented by Hafemeister and Flygare (HF) type potential. The consideration of Coulomb screening effect, which takes care of delocalized f-electron of the rare-earth atom, makes the present potential capable to explain various crystal properties more successfully. These interactions play important role in defining the crystal properties of heavy-earth compounds (HECs). We have derived and modified the expressions for elastic constants, which have been used to compute the structural phase transformation from B1 → B2 phase under the high pressure and other mechanical properties of these uranium compounds. The values of the phase-transition properties are in good agreement with experimental data and better than those obtained by earlier theoretical workers. The calculated values of Cauchy's discrepancy have shown a reasonably good agreement with the corresponding measured values.

We have also calculated the SOECs and their combinations (C_L, C_S and B_T), anisotropic factor, isotropic bulk, shear and Young's moduli and Kleinman parameter at ambient condition as well as at high pressures while TOECs and the first- and second-order pressure derivatives of SOECs at zero pressure. The thermophysical properties, i.e., Poisson's ratio (σ) and its volume derivative ($V(\mathrm{d}\sigma/\mathrm{d}V)$), the ratio of volume thermal expansion coefficient to specific heat (α_v/C_v), Debye temperature (θ_D) and Grüneisen parameter (γ) of these compounds have been calculated and they have shown a good agreement with the measured data.

Acknowledgement

The authors are thankful to DST, New Delhi for financial support.

References

[1] U. Benedict, J. Alloys Compd. 223 (1995) 216.
[2] T. Le Bihan, A. Bombardi, M. Idiri, S. Heathman, A. Lindbaum, J. Phys.: Condens. Matter 14 (2002) 10595.
[3] P.deV. DuPlessis, T.M. Holden, W.J.L. Buyers, J.A. Jackman, A.F. Murray, C.F. Van Doorn, J. Phys. C 18 (1985) 2809.
[4] J. Nevenschwander, H. Boppart, J. Schoenes, E. Voit, O. Vogt, P. Wachter, in: J. Schoenes (Ed.), 14 Journees des Actinides, Edigenossich Technische Hochchule, Zurich, 1984, p. 30.
[5] J.A. Jackman, T.M. Holden, W.J.L. Buyers, P.deV. DuPlessis, O. Vogt, G. Genossar, Phys. Rev. B 33 (1986) 7144.
[6] P.deV. DuPlessis, D.L. Tillwick, J. Appl. Phys. 50 (1979) 1834.
[7] G.H. Lander, W.G. Stirling, Phys. Rev. B 21 (1980) 436.
[8] J.S. Olsen, S. Stenstrup, L. Gerward, U. Benedict, J.C. Spirlet, G.D. Andreetti, J. Less Common Met. 98 (1984) 291.
[9] J.S. Olsen, L. Gerward, U. Benedict, J. Appl. Crystallogr. 18 (1985) 37.
[10] P.K. Jha, S.P. Sanyal, Phys. Rev. B 46 (1992) 3664.
[11] P.K. Jha, R.K. Singh, S.P. Sanyal, Physica B 174 (1991) 101.
[12] W.G. Stirling, G.H. Lander, O. Vogt, J. Phys. C 16 (1983) 4093.
[13] W.J.L. Buyers, A.F. Murray, T.M. Holden, E.C. Svensson, P.deV. DuPlessis, G.H. Lander, O. Vogt, Phys. Rev. B 102 (1980) 291.
[14] M.S.S. Brooks, J. Phys. F: Met. Phys. 14 (1984) 653.
[15] M. Erbudak, F. Meier, Physica B 102 (1980) 134 (and references therein).
[16] G.M. Lander, W.G. Stirling, J.M. Rossat-Mignod, M. Hagen, O. Vogt, Rev. B 41 (1990) 6899 (and references therein).
[17] A.L. Cornelius, J.S. Schilling, O. Vogt, K. Mattenberger, U. Benedict, J. Magn. Magn. Mater. 161 (1996) 169.
[18] A.K. Srivastava, S. Kumaria, B.R.K. Gupta, Phase Trans. 18 (2010) 28.
[19] B.R. Cooper, Y.-L. Lin, J. Appl. Phys. 83 (1998) 6432.
[20] B. Johansson, M.S.S. Brooks, in: K.A. Gschneidner Jr., L. Eyring, G.H. Lander, G.R. Choppin (Eds.), Handbook on the Physics and Chemistry of Rare Earths, vol. 17, Elsevier, Amsterdam, 1993.
[21] M.S.S. Brooks, B. Johansson, H.L. Skriver, in: A.J. Freeman, G.H. Lander (Eds.), Handbook on the Physics and Chemistry of the Actinides, vol. 1, North-Holland, Amsterdam, 1984.
[22] S. Durai, P. Babu, Bull. Mater. Sci. 28 (2005) 669.
[23] A. Gour, S. Singh, R.K. Singh, J. Alloys Compd. 468 (2009) 438.
[24] D. Varshney, N. Kaurav, R. Kinge, R.K. Singh, J. Phys.: Condens. Matter 19 (2007) 236204.
[25] D. Varshney, N. Kaurav, U. Sharma, R.K. Singh, J. Alloys Compd. 448 (2008) 250.
[26] D. Varshney, G. Joshi, N. Kaurav, R.K. Singh, J. Phys. Chem. Solids 70 (2009) 451.
[27] D. Varshney, G. Joshi, M. Varshney, N. Kaurav, S. Shriya, Phys. B: Condens. Matter 405 (2010) 1663.
[28] K. Motida, J. Phys. Soc. Jpn. 55 (1986) 1636.
[29] D.W. Hafemeister, W.H. Flygare, J. Chem. Phys. 43 (1965) 795.
[30] C. Kittel, Introduction to Solid State Physics, John Wiley & Sons, New York, 2004.
[31] D.C. Gupta, R.K. Singh, Phys. Rev. B 45 (1992) 7031.
[32] R.K. Singh, Phys. Rep. 85 (1982) 259.
[33] D.C. Wallace, Thermodynamics of Crystals, John Wiley & Sons, New York, 1972.
[34] W.A. Harrison, Electronic Structure and Properties of Solids: The Physics of the Chemical Bond, Dover Publication Inc., New York, 1989.
[35] W. Cochran, Crit. Rev. Solid State Sci. 2 (1971) 1.
[36] D.C. Gupta, S. Kulshrestha, J. Phys.: Condens. Matter 21 (2009) 436011.
[37] D.C. Gupta, Ph.D. Thesis, Barkatullah University, Bhopal, India, 1991.
[38] H. Rudigier, H.R. Ott, O. Vogt, Phys. Rev. B 32 (1985) 4584.